

Modeling of interior beam-column joints for nonlinear analysis of reinforced concrete frames



Zhangcheng Pan^{a,*}, Serhan Guner^b, Frank J. Vecchio^a

^a Department of Civil Engineering, University of Toronto, Toronto, ON M5S 1A4, Canada

^b Department of Civil Engineering, University of Toledo, OH 43607, United States

ARTICLE INFO

Article history:

Received 20 December 2016

Revised 26 March 2017

Accepted 28 March 2017

Available online 7 April 2017

Keywords:

Beam-column joints

Monotonic loading

Nonlinear analysis

Bond-slip

Shear deformation

Reinforced concrete frames

ABSTRACT

Beam-column connections undergo significant shear deformations and greatly contribute to story drifts during earthquake loading, yet their response is typically neglected in traditional frame analyses through the use of rigid end offsets. Although local joint models are available in the literature for the investigation of single, isolated joints, there is a lack of holistic frame analysis procedures simulating the joint behavior in addition to important global failure modes such as beam shear, column shear, column compression, and soft story failures. The objective of this study is to capture the impact of local joint deformations on the global frame response in a holistic analysis by implementing a joint model into a previously-developed global frame analysis procedure. The implemented joint element simulates the joint shear deformations and bar-slip effects. Concrete confinement effects are also considered so that both older and modern joints can be modeled. The developed procedure successfully captures the local load-deflection response of joints within a global frame analysis procedure. The ratio of predicted and observed peak load had a mean of 1.25 before the modification, and a mean of 1.05 after the modification.

© 2017 Elsevier Ltd. All rights reserved.

1. Introduction

According to the U.S. Geological Survey, at least 850,000 people were killed and more than 3 million buildings collapsed or were significantly damaged during the 26 major earthquake events that occurred over the past two decades [1]. Reinforced concrete frame structures constituted a large percentage of those buildings. Common failure modes observed after those earthquakes included beam-column joint shear, column shear, beam shear, column compression, reinforcement bond slip, foundation failures and soft story failures.

While most of the failure modes are commonly considered in typical frame analyses, the joint failure mode is often neglected. It is crucial to consider all modes since any one of them may govern the failure of the structure. The interaction among the failure modes should also be considered. In the traditional analysis of reinforced concrete frame structures subjected to seismic loading, beam-column joints are assumed rigid. This assumption implies that the joint core remains elastic and deforms as a rigid body throughout an earthquake event, even if the beams and columns undergo significant deformation and sustain severe damage. On

the contrary, tests on seismic performance of non-ductile beam-column joints conducted by Walker [2] have demonstrated that joint deformations due to shear cracking and bond slip are major contributors to lateral story drifts as shown in Fig. 1.

Although joint shear failure is a local failure mechanism, it often leads to progressive collapse of buildings. Insufficient anchorage lengths of reinforcing bars, unconfined connections, and deterioration of reinforced concrete materials are the main contributors to this type of failure, as illustrated in Fig. 2. Frame joints designed prior to the 1970s according to older design standards, with little or no transverse reinforcement, exhibit a non-ductile response and are more vulnerable to joint shear failures. Older design codes did not specify a limit on the joint shear stress or required joint transverse reinforcement prior to the pioneering experiment of Hanson and Connor [3]. As a result, joints in these frames exhibit high joint shear, which contribute to greater story drifts and higher bond stresses with potential bar slippage under seismic loading. Joints in newer buildings possess better reinforcement detailing with transverse reinforcement as specified in modern building design codes such as CSA A23.3-14 [4]. Nonetheless, tests have demonstrated that even newer joints exhibit shear cracking under strong seismic loading, significantly contributing to story drifts of the global structure [5].

Since the pioneering experiment of seismic resistance of beam-column joints conducted by Hanson and Connor in 1967 [3], there

* Corresponding author.

E-mail addresses: ryan.pan@mail.utoronto.ca (Z. Pan), serhan.guner@utoledo.edu (S. Guner), fjv@civ.utoronto.ca (F.J. Vecchio).

Nomenclature

A	transformation matrix that converts the nodal displacements to component deformations	v	internal nodal displacement
A_b	nominal bar area	\hat{w}	distance between the bar slip springs on the column side
d_b	nominal bar diameter	x	parameter that is a function of the strut strain
E_c	tangent modulus of elasticity of concrete	α_{strut}	angle of inclination of the strut
E_s	modulus of elasticity of steel	Δ	component deformations
E_{sec}	secant modulus of elasticity of concrete	Δ_{slip}	slip of the reinforcing bar at the joint interface
E_{sh}	hardening modulus of steel	ϵ_{cc}	strain of the confined concrete at the peak stress
f_{cc}^f	compressive strength of confined concrete	ϵ_t	principal tensile strain of concrete in the shear panel
f_i	component force	φ	interior nodal resultant
f_s	stress in the reinforcing steel at the interface of the joint	τ_{EC}	bond stress of elastic steel in compression
f_y	yield stress of steel	τ_{ET}	bond stress of elastic steel in tension
F	external nodal resultant	τ_{YC}	bond stress of post-yielding steel in compression
\hat{h}	distance between the bar slip springs on the beam side	τ_{YT}	bond stress of post-yielding steel in tension
k	confinement effectiveness coefficient	w_{strut}	in-plane width of the strut
r	parameter that is a function of the tangent and the secant modulus of elasticity of concrete		
u	external displacements and rotations		

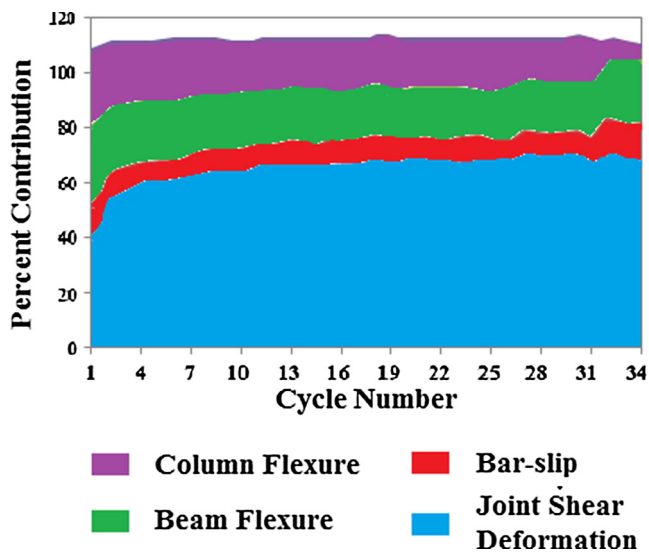


Fig. 1. Contributions of displacement factors to story drift for an older type joint, Specimen CD15-14, subjected to reversed cyclic loading [2].

has been an ongoing effort in understanding the behavior of beam-column joints under seismic actions, and in creating numerical simulation methods to model and determine joint response under

various loading conditions. Researchers have proposed a variety of beam-column joint models. These models can be categorized into three classes: rotational hinge models such as by Alath and Kunath [6], Altoontash [7] and Shin and LaFave [5]; component models such as by Youssef and Ghobarah [8], Lowes and Altoontash [9] and Mitra and Lowes [10]; and finite element models [11]. Each model has its advantages and limitations, and there is no scientific consensus on a model that is optimal for all applications. Rotational hinge models require calibration for each specific type of joint. Finite element models are complex and require significant computational resources; therefore, they are not suitable for holistic frame analyses. Component models provide a good balance between simplicity and accuracy. They are generally based on experimentally calibrated parameters, and they are suitable for analyzing large frames. They use mechanics-based formulations and generally do not require calibration for each particular joint type. However, the results obtained usually depend on the material models used for the joint element.

While existing joint models are effective for the investigation of single isolated joints, they do not consider the interactions between the joints and the other parts of the structure within a global frame analysis procedure. Therefore, there is a need to develop a holistic analysis procedure incorporating the joint response. The primary focus of this current study is to capture the impact of local joint deformations on the global frame response subjected to monotonic loading by implementing a new joint model into a previously-developed global frame analysis proce-



(a) Insufficient anchorage length (b) Unconfined connection (c) Poor coverage

Fig. 2. Different joint failure modes in reinforced concrete frames under earthquake loading (Google Images).

cedure. This study focuses on the monotonic response as a foundation to understand the performance of the implementation of the joint element. This study is exclusively focused on the modeling of interior beam-column joints because they are the most common type and require the most number of nodes and components for modeling. Exterior and knee joints may be modeled by modifying the interior joint formulations and disabling some of the components. With the implementation of a joint model, the global procedure being further developed is expected to provide a better overall load-deflection response including the local joint response. The global procedure will also be able to capture joint failures, which would otherwise not have been detected. The improved analysis procedure will allow for the analysis of modern buildings for performance-based earthquake engineering, and for analysis of older buildings to identify the buildings which are at the risk of collapse during a future earthquake.

2. Overview of the joint model

After review of the current state-of-the-art for the modeling of interior beam-column joints of reinforced concrete frame structures, the model proposed by Mitra and Lowes [10] was selected to be implemented in a previously-developed global frame analysis procedure. This is a four node, thirteen degree-of-freedom component model that consists of three components: (1) eight zero-length bar slip springs to simulate the strength and stiffness loss in the bond between the concrete and reinforcing bars; (2) four interface shear springs to simulate the shear transfer from beams and columns to the joint; and (3) a panel element to simulate shear deformations in the joint region (Fig. 3). This model represents the inelastic actions taking place in the joints including mechanisms of joint core shear resistance and bond slip response.

The solution of this model requires finding the component deformations and corresponding material state of the joint element. The joint element is formulated based on compatibility, equilibrium and constitutive relationships. Compatibility of the element requires the four external nodal displacements to be compatible with the thirteen component deformations according to Eq. (1). Equilibrium of the element needs to be satisfied at four external and four internal nodes according to Eq. (2). Constitutive relationships, which consist of a bond slip response and a joint shear response, relate the component deformations to the component forces.

$$[\Delta_{13 \times 1}] = [A_{13 \times 16}] \begin{bmatrix} u_{12 \times 1} \\ v_{4 \times 1} \end{bmatrix} \tag{1}$$

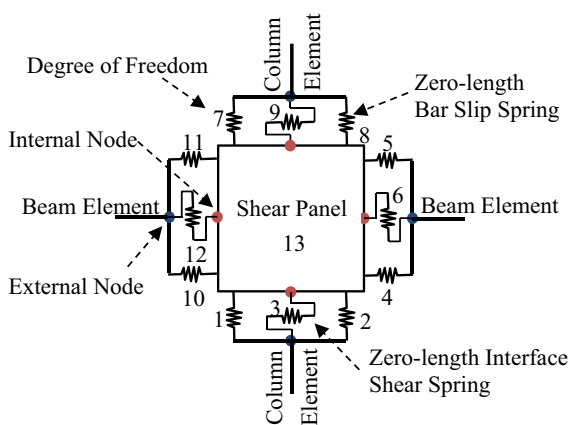


Fig. 3. Implemented interior beam-column joint model (from [10]).

$$\begin{bmatrix} F_{12 \times 1} \\ \varphi_{4 \times 1} \end{bmatrix} = [A_{16 \times 13}^T] [f_{13 \times 1}] \tag{2}$$

Bond slip is joint mechanism which refers to the movement of the longitudinal reinforcing steel with respect to the surrounding concrete due to deterioration of the bond strength between the two. The bar slip springs in the joint element are utilized to represent this action. The bond slip model used is based on the experimental data of Elgehausen et al. [12], and the assumption of uniform bond stress prior to yielding of the reinforcing steel and piecewise uniform after yielding (Fig. 4).

In this joint model, the joint shear is transferred via a concrete compression strut as shown in Fig. 5. The concrete strut is confined by the longitudinal reinforcing steel in the joint arising from the beam and column members framing into the joint, and the transverse reinforcement in the joint region. The stress-strain model proposed by Mander et al. [13] for the uniaxially confined concrete is employed to determine the stress in the strut. The compressive stress in the strut obtained from the stress-strain model is then adjusted to account for cracking due to the tensile straining in the orthogonal direction of the strut, or the “compression softening” effect.

3. Implementation

The selected interior joint model was implemented into an existing frame analysis procedure, VecTor5, which is a nonlinear analysis program for two-dimensional reinforced concrete frame structures developed at the University of Toronto [14–16]. The program has the ability to capture shear effects and significant second-order mechanisms. It includes a graphical pre-processor (FormWorks [17]) for users to create frame models, and a post-processor (Janus [18,19]) to visualize analysis results. Previous studies verified this procedure with over 100 experimental specimens and demonstrated that the program was able to accurately simulate the nonlinear behavior of frames [15,16,20–22]. The program currently uses semi-rigid end offsets to model joints. The objective of this joint element implementation is to replace all members and nodes within the joint core region with a single joint element. The expected end result of this implementation is improved modeling of both local joint and global frame responses. Refer to the thesis “Modeling of Interior Beam-Column Joints for Nonlinear Analysis of Reinforced Concrete Frames” by Pan [23] for more details on the implementation and the formulations.

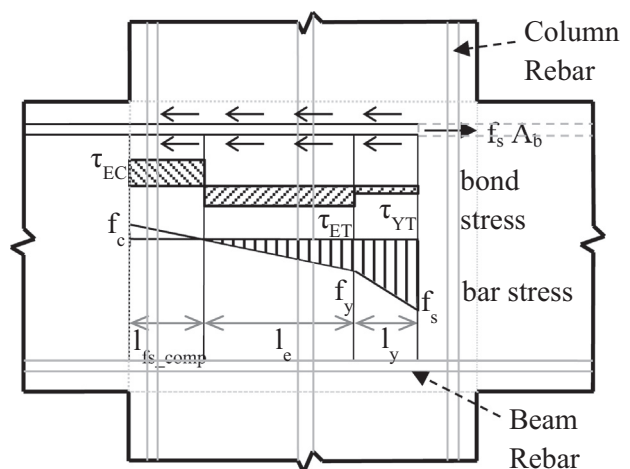


Fig. 4. Bond stress and bar stress distribution along a reinforcing bar anchored in a joint.

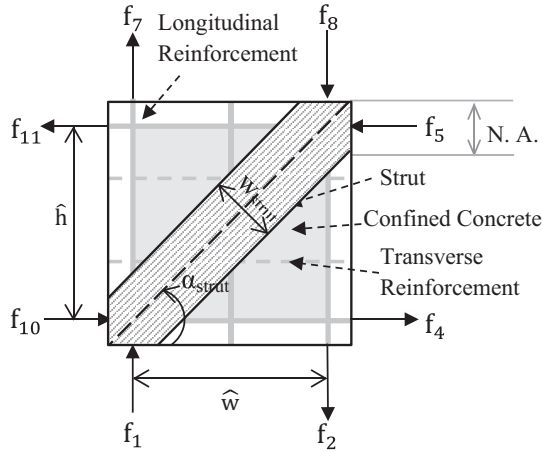


Fig. 5. Idealized diagonal concrete compression strut model.

3.1. Global frame modeling

The procedure divides a frame model into a finite number of members. For each member, a layered (fiber) analysis technique is employed for the nonlinear sectional analysis. Each concrete and steel layer is analyzed individually based on the Disturbed Stress Field Model (DSFM) [24]. Fig. 6 illustrates the joint element implementation in the global procedure. The members in the joint region are replaced with a beam-column joint element.

The global analysis procedure starts with reading four input text files consisting of structure, load, job and auxiliary files. These files define the geometry of the structure, material properties, loading data, analysis parameters, material behavior models and other general parameters. The load vector and the stiffness matrix are assembled. A global analysis of the frame is performed to determine nodal displacements, nodal reactions and member end actions. The geometry of the frame is updated based on the computed nodal displacements. The procedure determines the axial and shear strain distributions through the depth of each member, and performs nonlinear sectional analysis iterations to calculate the sectional forces. The unbalanced forces, or the difference between the global and sectional forces, are calculated for each member, and added to the compatibility restoring forces to be applied to the frame in the next iteration. The calculations for the nonlinear sectional analysis are repeated until all unbalanced forces become zero or the number of maximum iterations is reached. Finally, the results obtained for the current load stage are stored in an output text file before proceeding to the next load stage. Although the implementation of the joint element does not change these basic analysis steps of the global procedure, it requires new subroutines for the local joint analysis as well as modifications of the global analysis procedure, which are the main focus of this paper.

3.2. Local joint element

The local joint element subroutine was constructed based on the component model. Fig. 7 shows a flowchart of the solution process for the joint element. This iterative solution process includes the following five steps:

- (1) Obtain the material properties, geometric properties and other relevant parameters from the global procedure.

- (2) Perform sectional analysis to determine the nominal flexural strength for the beam and column elements that frame into the joint. For this strength calculation, it is assumed that the beams carry zero axial load. A linear axial strain distribution is assumed through the height of the section with the strain at the extreme compression fiber taken as -0.003 .
- (3) Determine the transformation matrix and component deformations. The transformation matrix is a function of the joint geometry and the distance between the bar slip springs on each face of the joint element.
- (4) Determine the corresponding force resultants, shear equivalent moments, and component stiffnesses for all 13 components. The force resultants and stiffnesses of the bar slip springs are computed in the bar slip spring subroutine. The shear equivalent moments and stiffnesses of joint panel are computed in the shear panel subroutine. The interface shear springs are assumed to remain stiff and elastic.
- (5) Check whether the convergence criteria are satisfied.

In order to achieve the state of convergence, the squared internal nodal force resultants must be less than the tolerance. The tolerance was set as 1 kN^2 in the algorithm. If convergence is not achieved, new component deformations are calculated and the same solution process is repeated until the limit on the maximum number of iterations is reached.

The joint analysis returns a joint analysis matrix to the global procedure, and stores the joint analysis results as a data file for inspection. The stiffness matrix of the joint element with the size of 16 by 16 is calculated based on the component stiffness. Instead of using the tangent stiffness, the component secant stiffness is used to avoid getting large stiffness values at low component deformations. The stiffness matrix is condensed with respect to the four exterior nodes (i.e. the first 12 degrees-of-freedom) using the partitioned matrix and static condensation. The condensed matrix, with the dimension of 12 by 12, is then projected to a joint analysis matrix, which has the same size as the global stiffness matrix (Fig. 8).

For frames with multiple interior joints, condensed stiffness matrices are determined for individual joints which are translated into a large joint analysis matrix. The results from the analysis include cracking parameters, joint core parameters, reinforcing steel parameters and joint panel coordinates. All parameters are computed in the bar slip spring subroutine and the shear panel subroutine.

3.3. Bar slip spring

The bar slip springs subroutine was constructed based on the bar stress versus slip relationship according to Eq. (3).

$$\Delta_{slip} = 2 \frac{\tau_E}{E_s} \frac{l_s^2}{d_b} \quad \text{for } f_s < f_y \quad (3a)$$

$$\Delta_{slip} = 2 \frac{\tau_E}{E_s} \frac{l_e^2}{d_b} + \frac{f_y l_y}{E_s} + 2 \frac{\tau_Y}{E_{sh}} \frac{l_y^2}{d_b} \quad \text{for } f_s \geq f_y \quad (3b)$$

where $l_s = \frac{f_s}{\tau_E} \frac{A_b}{\pi d_b} l_e = \frac{f_y}{\tau_E} \frac{A_b}{\pi d_b} l_y = \frac{f_s - f_y}{\tau_Y} \frac{A_b}{\pi d_b}$.

Properties of the longitudinal reinforcement and the surrounding concrete are input to this subroutine. The algorithm takes the input spring deformation and calculates the corresponding spring force and secant stiffness. The bar stress versus slip curve is divided into four segments: elastic tension, post-yielding tension, elastic compression, and post-yielding compression. The secant stiffness is defined as the force resultant divided by the spring deformation.

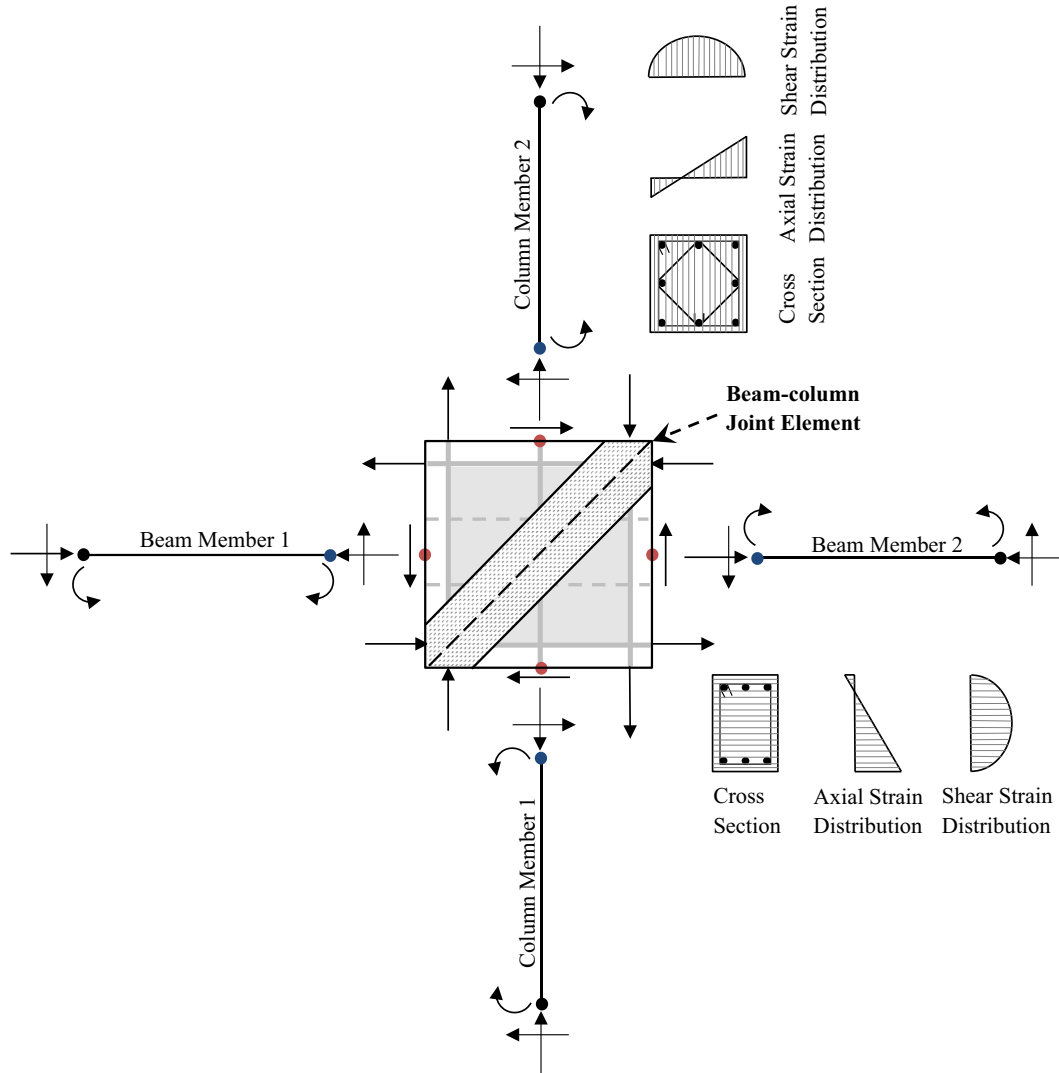


Fig. 6. Joint element implementation in the global procedure.

Rebar end stresses and slips are calculated as a part of the joint analysis results in the output files for users.

3.4. Shear panel

The shear panel subroutine was constructed based on the Mander et al. model [13] for uniaxial confined concrete according to Eq. (4), with a reduction factor proposed by Mitra and Lowes [10].

$$f_{cc} = \frac{f'_{cc} \chi r}{r - 1 + \chi'} \tag{4}$$

where $\chi = \frac{\epsilon_{strut}}{\epsilon_{cc}}$ and $r = \frac{E_c}{E_c - E_{sec}}$.

The reduction factor is given by Eq. (5) for joints with transverse reinforcement and Eq. (6) for joints without transverse reinforcement.

$$\frac{f_{cstrut}}{f_{cMander}} = 3.62 \left| \frac{\epsilon_t}{\epsilon_{cc}} \right|^2 - 2.82 \left| \frac{\epsilon_t}{\epsilon_{cc}} \right| + 1 \text{ for } \left| \frac{\epsilon_t}{\epsilon_{cc}} \right| < 0.39 \tag{5a}$$

$$\frac{f_{cstrut}}{f_{cMander}} = 0.45 \text{ for } \left| \frac{\epsilon_t}{\epsilon_{cc}} \right| \geq 0.39 \tag{5b}$$

$$\frac{f_{cstrut}}{f_{cMander}} = 0.36 \left| \frac{\epsilon_t}{\epsilon_{cc}} \right|^2 - 0.60 \left| \frac{\epsilon_t}{\epsilon_{cc}} \right| + 1 \text{ for } \left| \frac{\epsilon_t}{\epsilon_{cc}} \right| < 0.83 \tag{6a}$$

$$\frac{f_{cstrut}}{f_{cMander}} = 0.75 \text{ for } \left| \frac{\epsilon_t}{\epsilon_{cc}} \right| \geq 0.83 \tag{6b}$$

The algorithm takes the input panel shear deformation and calculates the corresponding shear equivalent moment and secant stiffness values. The secant stiffness is defined as the shear equivalent moment divided by the panel shear deformation. The new procedure calculates the cracking angle, the mean crack spacing and the mean crack width.

3.5. Modifications of the global frame analysis procedure

In order to integrate the local joint element into the global frame analysis procedure, proper modifications to two components of the global frame analysis procedure are necessary. The first component is the detection of the interior joints. In this algorithm, an interior joint node is labelled as such if the node is associated with four in-framing members. Similarly, an exterior joint node has three members framing into it, whereas a knee joint node has two members framing into it.

The next step is the assembly of the global stiffness matrix. A revised method is proposed to locate the replacement of the existing beam and column members in the joint region for the joint elements. In the original algorithm, stiffness matrices for individual

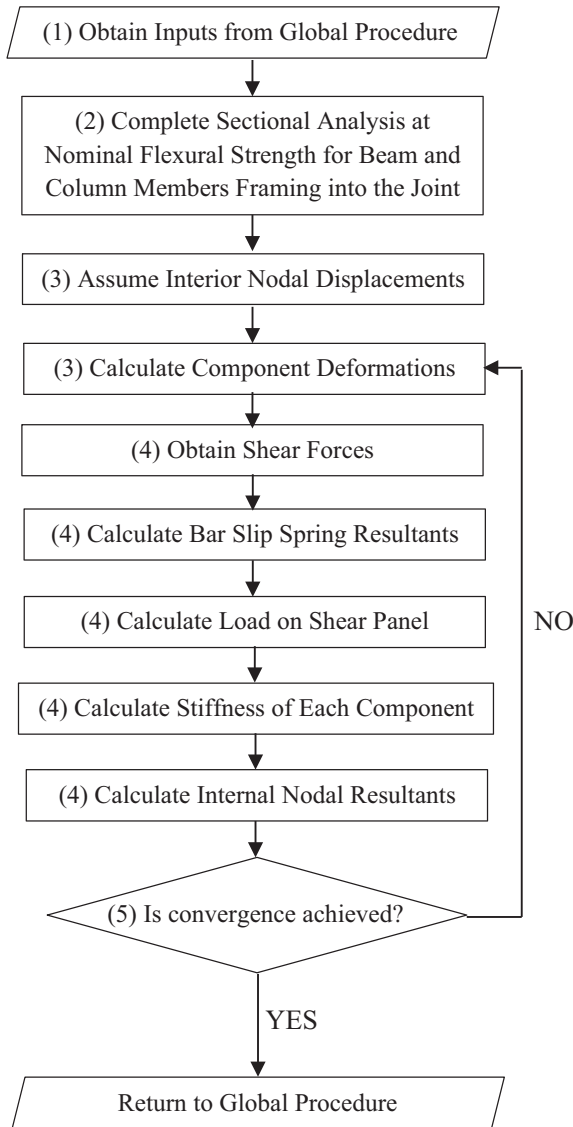


Fig. 7. Flowchart of solution process for the joint element [9]

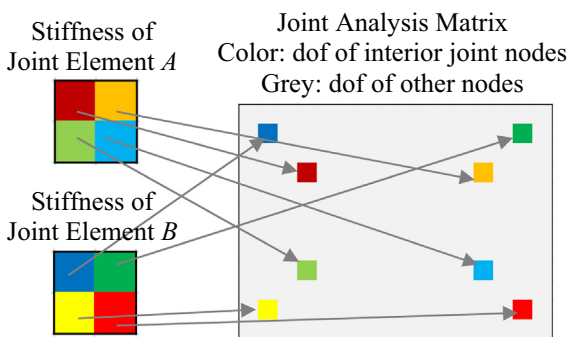


Fig. 8. Joint analysis matrix for frames with multiple interior joints.

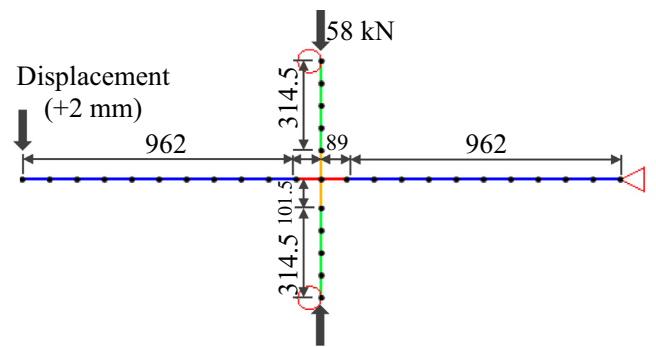
members are assembled into the global stiffness matrix. The new algorithm detects the joint nodes and replaces four members in the joint regions with joint elements. The joint analysis matrix is added to the member stiffness matrix for the assembly of the global stiffness. Because of the replacement of the interior joint nodes, the size of the global stiffness matrix is reduced by a degree of

three for each interior joint detected. The size of the load and the displacement vectors is also adjusted to reflect the removal of the joint nodes.

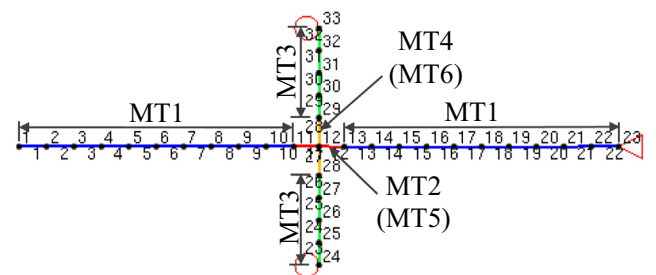
4. Experimental validation

In order to validate the resulting global frame analysis procedure, nine interior beam-column subassemblies from four different experimental studies available in the literature were selected. The interior beam-column subassemblies considered include: two specimens tested by Shiohara and Kusuhara [25], two specimens tested by Park and Dai [26], two specimens tested by Noguchi and Kashiwazaki [27], and three specimens tested by Attaalla and Agbabian [28]. The specimens considered cover various material properties, reinforcing ratios, and failure mechanisms. Analyses were performed using alternately the semi-rigid joints and the new joint element. All analysis options and material behavior models used were kept identical, with the only difference being the joint models. Monotonic analyses were performed to determine the backbone curve for the hysteretic responses. In addition, three large-scale frame structures with different joint reinforcement ratios were selected for evaluation and verification. Refer to the thesis “Modeling of Interior Beam-Column Joints for Nonlinear Analysis of Reinforced Concrete Frames” by Pan [23] for more details on the experimental validation.

The subassembly with the best prediction was Specimen SHC2 from the tests conducted by Attaalla and Agbabian. Fig. 9 shows the analytical model of Specimen SHC2 including loading, support restraints and material types used in the model. Fig. 10 shows the experimental and analytical responses of Specimen SHC2 which had two transverse ties in the joint core. The failure of the subassembly was mainly due to the shear mechanism in the joint core, but damage in the beams close to the column faces was also noticeable. The peak load was 16.7 kN at a displacement of



(a) Dimensions, loading and support restraints of Specimen SHC2



(b) Material types of Specimen SHC2

Fig. 9. Analytical model of Specimen SHC2.

100 mm. The longitudinal reinforcement of the beams yielded at the joint interface at a displacement of 28 mm. The maximum shear stress of the joint panel was 7.24 MPa with the corresponding maximum shear distortion of 8.7×10^{-3} . The analysis with the new joint element predicted the failure mechanism as beam yielding followed by joint failure, matching well with the experimental observations. The analysis using semi-rigid joints, on the other hand, predicted the failure mechanism due to beam yielding. The analysis with new joint element predicted a peak load of 18.4 kN at a displacement of 86 mm. The longitudinal reinforcement of the beam yielded at the left column interface at a displacement of 38 mm. The transverse reinforcement yielded at a displacement of 66 mm, when the structure started losing its strength and the load slowly declined. The maximum shear stress of 5.8 MPa was reached at a displacement of 82 mm with the corresponding shear strain of 12.2×10^{-3} . The average crack width was 1.4 mm at this time.

The analysis using semi-rigid joints predicted a load capacity of 21.6 kN at a displacement of 100 mm. The longitudinal reinforcement of the beam yielded at a displacement of 20 mm. The column steel yielded at a displacement of 44 mm. Flexural cracking in the beams close to the joint panel was noticeable at a displacement of 100 mm. The joint was in good condition without noticeable shear cracking. A comparison of the observed and predicted cracking patterns is shown in Fig. 11. In conclusion, the analytical response predicted by the modified procedure was a good match for the experimental results in terms of the peak load and the stiffness of the subassembly. The modified procedure successfully captured the failure mechanism as beam yielding followed by joint failure. The response of the joint shear panel was predicted reasonably well.

The subassembly with the least accurate prediction was Specimen A1 from tests conducted by Shiohara and Kusuhara. Fig. 12 shows the experimental and analytical response of Specimen A1. In the experiment, the beam yielded at a displacement of 21 mm, where the face rotation of the joint panel suddenly increased, greatly contributing to the overall displacement of the subassembly. At a displacement of 29 mm, the concrete crushed at the beam-joint interface, and the concrete cover started spalling off from the joint panel. At a displacement of 44 mm, the concrete cover spalled off thoroughly, which exposed the ties.

As observed from Fig. 12, the analysis using semi-rigid joints overestimated the stiffness and strength of the subassembly by 24%. The analysis with the new joint element, on the other hand,

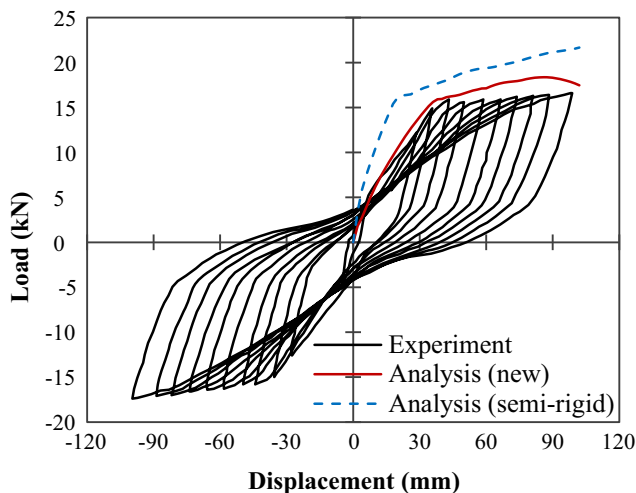
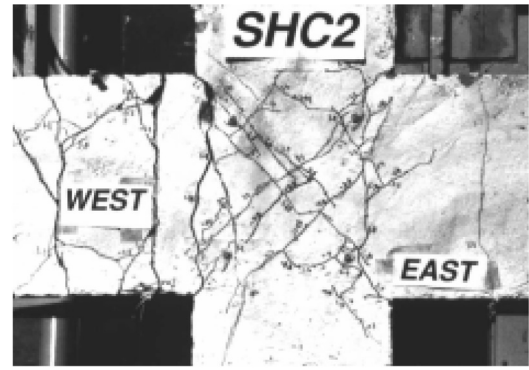
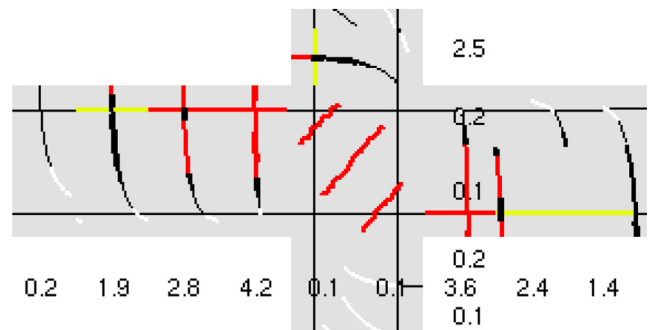


Fig. 10. Comparison of the load-displacement response of Specimen SHC2.



(a) Observed cracking pattern



(b) Predicted cracking pattern

Fig. 11. Cracking pattern of Specimen SHC2.

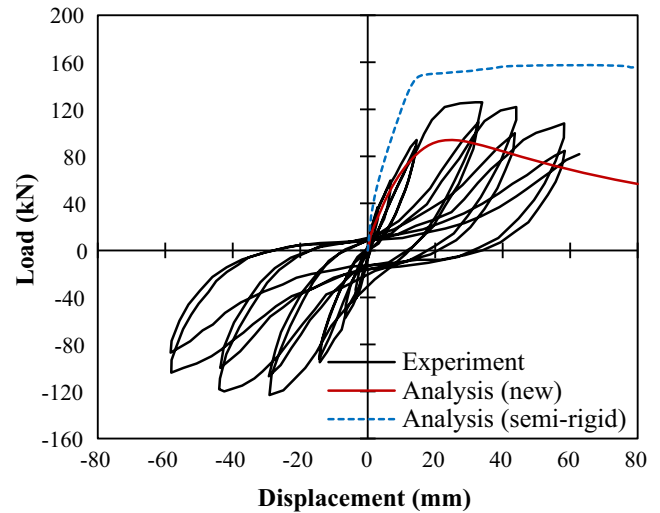


Fig. 12. Comparison of the load-displacement response of Specimen A1.

underestimated the strength of the subassembly by 26%, but the stiffness and the shape of the response curve were predicted better. The modified procedure predicted a joint failure without yielding of the beam reinforcement, whereas the specimen exhibited a failure mechanism of beam yielding followed by joint failure in the experiment. The shear panel reached its peak stress of 3.70 MPa at a displacement of 26 mm, when the subassembly reached its peak load of 93.2 kN. The average crack width in the joint panel at a displacement of 60 mm was determined as 5.5 mm.

On the contrary, the analysis using semi-rigid joints predicted failure due to beam yielding. It also predicted beam yielding at

the joint interface at a displacement of 13 mm. Flexural cracks initiated in beam members adjacent to the joint propagated with increasing applied displacement. Cracking in the joint panel was relatively insignificant. Overall, neither of the predictions was a good match with the experimental response. One possible reason for the divergence between the experimental and analytical responses could be the inaccurate estimation of the confinement coefficient of the joint. The modified procedure provided a slightly better prediction by identifying the joint failure and the subsequent loss of stiffness. The modified procedure also provided a good prediction on the concrete response of the joint core.

With the new joint element, the global analysis procedure was able to provide better predictions in terms of failure mechanism and peak loads. For the nine interior joint subassemblies modeled, the ratio of predicted to observed peak load had a mean of 1.05 and a coefficient of variation of 18.3%. Table 1 summarizes the properties of interior beam-column subassemblies modeled in this study. Table 2 summarizes the analytical results of the simulations. In Table 2, “VT5/Exp.” refers to the results using the original procedure.

5. Parametric studies

Parametric studies were carried out to investigate the impact of four parameters on the load-displacement response of the subassemblies. These parameters include: loading type, confinement, compression softening, and bond stress. In this section, parameters associated with confinement, compression softening, and bond stress were studied based on the comparisons of the load-displacement responses of Specimen SHC2. The impact of the loading type was studied in order to understand whether the backbone curve of the cyclic response was a good representation of the monotonic response. Fig. 13 shows a comparison of the analytical load-displacement responses of Specimen A1 subjected to monotonic loading and reversed cyclic loading. In this example, the monotonic response curve was shown to be capable of capturing the initial and post-yielding stiffness of the reversed cyclic response. The peak loads and the load at first beam yielding simulated under the monotonic and reversed cyclic loading conditions were also similar. The comparison shows that the backbone curve of the reversed cyclic response was a good representation of the monotonic response in terms of the peak load and the initial stiffness of the structure. However, the loss of stiffness due to the hysteretic response may not be captured by the monotonic response.

The second parameter studied was the impact of the confinement effectiveness coefficient which considers the confinement in the column section as well as the confinement contributed by the transverse reinforcement in the joint core. The value of 1.0 represents a fully confined joint core, whereas the value of 0.0 represents a joint with no transverse reinforcement. The subassemblies were modeled under these two conditions and the load-displacement responses were compared to the original analytical response as shown in Fig. 14(a). The coefficient was found to be 0.189 for the specimen in this case. It was observed that confinement of the transverse reinforcement delayed concrete crushing of the joint core and provided greater strength for the subassemblies that exhibited significant joint damage.

The next parameter investigated was the impact of the reduction factor due to the compression softening effect. The reduction factor of 1.0 represents no strength reduction due to joint cracking. As shown in Fig. 14(b), the response for a reduction factor of 1.0 is very close to the response from the original procedure with semi-rigid end offsets, as expected. This confirmed the influence of the compression softening in the new model.

The last parameter examined was the bond stress. In order to assess the impact of the bond stress on the load-displacement response, the bi-uniform bond stresses proposed by Sezen and Moehle [29] were employed and tested. A comparison of the responses shown in Fig. 14(c) concluded that the assumption of the bond stresses did not have a significant impact on the global load-displacement response for the subassemblies. This may be explained by the observation that the subassemblies did not exhibit major bond damage or failure during the tests.

6. Summary and conclusions

6.1. Summary

An interior beam-column joint model was implemented into a previously-developed global frame analysis procedure, VecTor5. The implemented joint element enabled the consideration of joint shear actions and bond slip effects taking place inside interior joint cores. This allowed for improved simulations of global load-deflection response and local joint conditions for beam-column subassemblies and frames subjected to monotonic loading conditions.

The analysis procedure with the new joint element was verified with nine interior beam-column joint subassemblies. As the main

Table 1
Summary of the properties of interior beam-column subassemblies.

Specimen	Shiohara and Kusahara [25]		Park and Dai [26]		Noguchi and Kashiwazaki [27]		Attaalla and Agabian [28]		
	A1	D1	U1	U2	OKJ2	OKJ6	SHC1	SHC2	SOC3
<i>(a) Beam properties</i>									
Top Reinforcement	8-D13	6-D13	5-D16	2-D28	9-D13	8-D13	3-D10	3-D10	3-D10
Bottom Reinforcement	8-D13	6-D13	2-D16	2-D20	7-D13	7-D13	3-D10	3-D10	3-D10
Transverse Reinforcement	D6@50	D6@50	Various	Various	D6@50	D6@50	D6@72	D6@72	D6@72
<i>(b) Column properties</i>									
Longitudinal Reinforcement	16-D13	14-D13	8-D16	8-D20	20-D13	20-D13	4-D13	4-D13	4-D13
Transverse Reinforcement	D6@50	D6@50	Various	Various	D6@40	D6@40	D6@51	D6@51	D6@51
<i>(c) Joint properties</i>									
Concrete strength (MPa)	28.3	30.4	45.9	36.0	70.0	53.5	56.5	59.5	47.2
Height (mm)	300	300	457	457	300	300	203	203	203
Width (mm)	300	300	406	406	300	300	178	178	178
Thickness (mm)	300	300	305	305	300	300	127	127	127
Trans. reinforcement	5-D6	5-D6	5-D12/8	5-D12	6-D6	6-D6	1-D6	2-D6	2-D6
Confinement coefficient	0.725	0.702	0.560	0.570	0.786	0.786	0.102	0.189	0.187

Table 2
Summary of the analytical results of interior beam-column subassemblies.

Results		Shiohara and Kusahara [25]		Park and Dai [26]		Noguchi and Kashiwazaki [27]		Attaalla and Agbabian [28]		
		A1	D1	U1	U2	OKJ2	OKJ6	SHC1	SHC2	SOC3
Failure mechanism	Analysis	JF	JF	BY	BY	BY	BY	BYJF	BYJF	BYJF
	Experiment	BYJF	BYJF	BY	BY	BYJF	JF	BYJF	BYJF	BYJF
Peak load (kN)	Analysis	94.0	112.7	94.7	132.7	265.6	264.2	16.38	18.36	15.65
	Experiment	126.6	133.9	80.0	111.0	237.0	214.0	16.02	16.73	16.02
	Anly./Exp.	0.74	0.84	1.18	1.20	1.12	1.23	1.02	1.10	0.94
	VT5/Exp.	1.24	1.22	1.18	1.29	1.16	1.25	1.34	1.29	1.26
Load at first beam yielding (kN)	Analysis	N/A	N/A	67.6	50.6	245.9	248.2	15.91	15.59	15.47
	Experiment	118.6	89.7	54.2	78.9	237	N/A	11.90	12.20	13.40
	Anly./Exp.	N/A	N/A	1.25	0.64	1.04	N/A	1.34	1.30	1.15
	VT5/Exp.	1.19	1.49	1.32	1.29	1.02	N/A	1.30	1.32	1.20

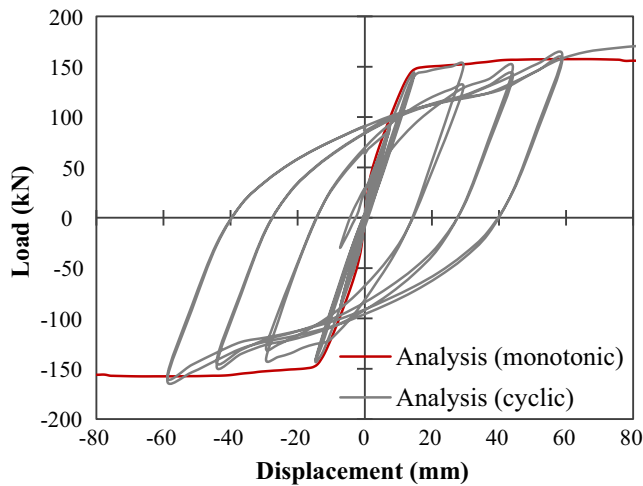


Fig. 13. Comparison of the load-displacement responses of Specimen A1.

focus of the verification was to determine the accuracy of the implementation and the improvements over the original program, the specimens considered covered various material properties, reinforcing ratios and failure mechanisms. The analytical responses of the specimens were compared to the experimental responses in terms of load-displacement responses, failure modes, peak loads, loads at first beam yielding, crack widths, and joint panel shear distortions.

6.2. Conclusions

Based on the results of the analyses performed, the following conclusions and observations are reached:

- Beam-column joint deformations due to shear cracking and bond slip are major contributors to lateral story drifts. It is crucial to consider the local joint response in frame analysis.
- There is a lack of global frame analysis procedures capturing the joint behavior in addition to important global failure modes. If the joint response is neglected, joint deformations and failures will not be captured.
- Component-based joint models are suitable for implementation into nonlinear fiber-based frame analysis procedures. Modifications of the global frame analysis procedure, including the detection of the interior joints and the assembly of the global stiffness matrix, are required for this implementation.
- This study modified an existing distributed plasticity, fiber element frame analysis procedure to incorporate the local joint response. Nine specimens of interior beam-column subassemblies were modeled. The ratio of predicted and observed peak load had a mean of 1.25 before the modification, and a mean of 1.05 after the modification. In addition, the predicted failure mechanisms, shear panel distortions, and average crack widths for the specimens showed good correlations with the experimental results.
- The compression softening model exerts a significant influence on the predicted load-displacement response. This is concluded from a parametric study of the impact of the reduction factor

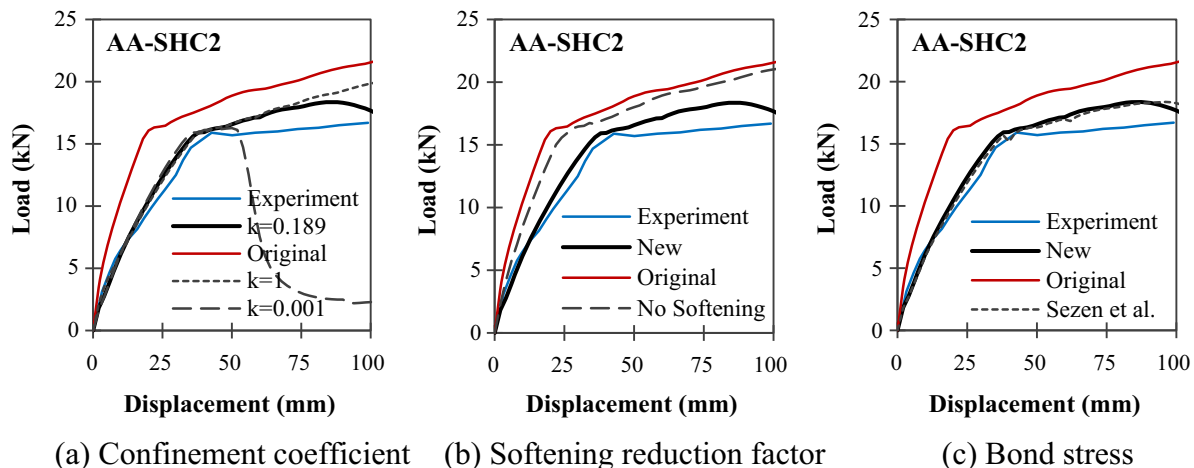


Fig. 14. Comparison of the load-displacement responses of Specimen SHC2.

due to the compression softening effect. Meanwhile, the new procedure captures the effects of concrete confinement and bar slippage, which are also influential factors that may be detrimental for the joint resistance mechanisms.

- The joint implementation is currently only applicable to interior joints subjected to monotonic loading. To extend the formulation to exterior and knee joints, new transformation matrices are required to define the equilibrium and compatibility relationships. To extend the formulation to reversed cyclic loading, hysteresis models and damage parameters must be considered.

Acknowledgements

Financial support provided by the Natural Sciences and Engineering Research Council of Canada (NSERC) and the Ontario Graduate Scholarship is gratefully acknowledged.

References

- [1] USGS. U.S. Geological Survey: Earthquakes with 1000 or More Deaths 1900–2014; 2014 <http://earthquake.usgs.gov/earthquakes/world/world_deaths.php> [Last Accessed September 18, 2016].
- [2] Walker SG. Seismic performance of existing reinforced concrete beam-column joints MS thesis. Washington: University of Washington, Seattle; 2001.
- [3] Hanson HW, Connor HW. Seismic resistance of reinforced concrete beam-column joints. *J Struct Eng Div, ASCE* 1967;93(ST5):533–59.
- [4] Concrete Design Handbook. 4th ed. Ottawa, ON: The Cement Association of Canada; 2014.
- [5] Shin M, LaFave JM. Modeling of cyclic joint shear deformation contributions in RC beam-column connections to overall frame behavior. *Struct Eng Mech* 2004;18(5):645–69.
- [6] Alath S, Kunnath SK. Modeling inelastic shear deformation in RC beam-column joints. Proc., 10th Conf., University of Colorado at Boulder, Boulder, Colo., May 21–24, vol. 2. New York: ASCE; 1995. p. 822–5.
- [7] Altoontash A. Simulation and damage models for performance assessment of reinforced concrete beam-column joints Ph. D. Thesis. California, United States: Department of Civil and Environmental Engineering, Stanford University; 2004.
- [8] Ghobarah A, Youssef M. Modeling of RC beam-column joints and structural walls. *J Earthquake Eng* 2001;5(1):91–111.
- [9] Lowes LN, Altoontash A. Modeling reinforced concrete beam-column joints subjected to cyclic loading. *J Strut Eng* 2003;129(12):1686–97.
- [10] Mitra N, Lowes LN. Evaluation, calibration, and verification of a reinforced concrete beam-column joint model. *J Strut Eng* 2007;133(1):105–20.
- [11] Eligehausen R, Genesio G, Ozbolt J, Pampanin S. 3D analysis of seismic response of RC beam-column exterior joints before and after retrofit. *Concr Repair, Rehab, Retrofitting* 2008;11:407–8.
- [12] Eligehausen R, Popov EP, Bertero VV. Local bond stress-slip relationship of deformed bars under generalized excitations EERC Report 83/23. Berkeley: University of California; 1983.
- [13] Mander JB, Priestley MJN, Park R. Theoretical stress-strain model for confined concrete. *J Strut Eng* 1988;114(8):1804–26.
- [14] Guner S. Performance assessment of shear-critical reinforced concrete plane frames Ph.D. Thesis. Department of Civil Engineering, University of Toronto; 2008. p. 429.
- [15] Guner S, Vecchio FJ. Pushover analysis of shear-critical frames: formulation. *Am Concr Inst Struct J* 2010;107(1):63–71.
- [16] Guner S, Vecchio FJ. Pushover analysis of shear-critical frames: verification and application. *Am Concr Inst Struct J* 2010;107(1):72–81.
- [17] Wong PS, Trommels H, Vecchio FJ. VecTor2 & FormWorks User's Manual. Online Publication; 2016. 347 pp <http://www.civ.utoronto.ca/vector/user_manuals/manual1.pdf>.
- [18] Loya, A.S., Guner, S., Vecchio, F.J. User's Manual of Janus for VecTor5. Online Publication; 2016, 17 pp. <<http://www.utoledo.edu/engineering/faculty/serhan-guner/Publications.html>>.
- [19] Chak I. Janus: A Post-Processor for VecTor Analysis Software MASC thesis. Toronto, Ontario, Canada: University of Toronto; 2013.
- [20] Guner S, Vecchio FJ. Analysis of shear-critical reinforced concrete plane frame elements under cyclic loading. *J Struct Eng, Am Soc Civil Eng* 2011;137(8):834–43.
- [21] Guner S, Vecchio FJ. Simplified method for nonlinear dynamic analysis of shear-critical frames. *Am Concr Inst Struct J* 2012;109(5):727–37.
- [22] Guner S. Simplified modeling of frame elements subjected to blast loads. *Am Concr Inst Struct J* 2016;113(2):363–72.
- [23] Pan Z. Modeling of interior beam-column joints for nonlinear analysis of reinforced concrete frames MASC thesis. Toronto, Ontario, Canada: University of Toronto; 2016.
- [24] Vecchio FJ. Disturbed stress field model for reinforced concrete: formulation. *ASCE J Struct Eng* 2000;126(8):1070–7.
- [25] Shiohara H, Kusahara F. Benchmark test for validation of mathematical models for non-linear and cyclic behavior of R/C beam-column joints. *ACI Spring Convention 2007*, Atlanta, United States; 2007.
- [26] Park R, Dai R. A comparison of the behavior of reinforced concrete beam-column joints designed for ductility and limited ductility. *Bull New Zealand Natl Soc Earthq Eng* 1988;21(4):255–78.
- [27] Noguchi H, Kashiwazaki T. Experimental studies on shear performances of RC interior beam-column joints. In: 10th World Conf. on Earthquake Engineering, Madrid, Spain. p. 3163–8.
- [28] Attaalla SA, Agbalian MS. Performance of interior beam-column joints cast from high strength concrete under seismic loads. *Adv Struct Eng* 2004;7(2):147–57.
- [29] Sezen H, Moehle JP. Bond-slip behavior of reinforced concrete members. In: *FIB – Symposium (CEB-FIP); Concrete Structures in Seismic Regions*, 6–9 May 2003. Athens, Greece.